

See discussions, stats, and author profiles for this publication at: <https://www.researchgate.net/publication/266386550>

# Detailed Structure Analysis of Atomic Positions and Defects in Zirconium Metal–Organic Frameworks

ARTICLE in CRYSTAL GROWTH & DESIGN · OCTOBER 2014

Impact Factor: 4.89 · DOI: 10.1021/cg501386j

CITATIONS

16

READS

164

7 AUTHORS, INCLUDING:



**Sigurd Øien**

University of Oslo

8 PUBLICATIONS 23 CITATIONS

SEE PROFILE



**Helge Reinsch**

University of Oslo

29 PUBLICATIONS 260 CITATIONS

SEE PROFILE



**Carlo Lamberti**

Università degli Studi di Torino

379 PUBLICATIONS 13,123 CITATIONS

SEE PROFILE



**Karl Petter Lillerud**

University of Oslo

146 PUBLICATIONS 5,525 CITATIONS

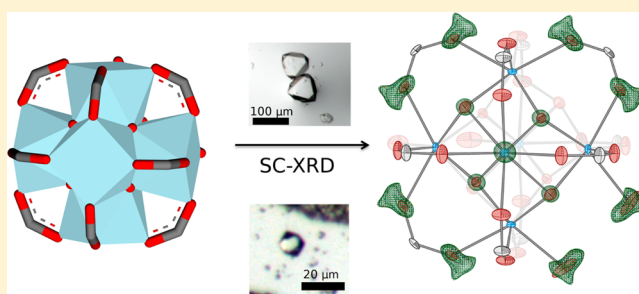
SEE PROFILE

## Detailed Structure Analysis of Atomic Positions and Defects in Zirconium Metal–Organic Frameworks

Sigurd Øien,<sup>†</sup> David Wragg,<sup>†</sup> Helge Reinsch,<sup>†</sup> Stian Svelle,<sup>†</sup> Silvia Bordiga,<sup>†,‡</sup> Carlo Lamberti,<sup>‡,§</sup> and Karl Petter Lillerud<sup>\*,†</sup><sup>†</sup>Department of Chemistry, University of Oslo, N-0371 Oslo, Norway<sup>‡</sup>Department of Chemistry, NIS and INSTM Reference Centre, Via Quarello 15, I-10135 Torino, Italy<sup>§</sup>Southern Federal University, Zorge Street 5, 344090 Rostov-on-Don, Russia

## S Supporting Information

**ABSTRACT:** We report the structure of the Zr metal–organic frameworks (MOFs) UiO-66 and UiO-67 to very fine detail using synchrotron single-crystal X-ray diffraction and the synthesis method used to obtain single crystals. Zr terephthalate MOF UiO-66 is known to have missing linkers, and the nature of these are shown to be coordinating water and solvent molecules. Single crystals of the isoreticular material UiO-67 does not show such missing linker defects.



Zr-based metal–organic frameworks (MOFs) are notable porous materials that recently have gained a lot of attention due to their properties as catalysts,<sup>1,2</sup> sensor materials,<sup>3</sup> and adsorbents.<sup>4</sup> They consist of discrete  $\text{Zr}_6\text{O}_4(\text{OH})_4$  clusters linked by polycarboxylates, creating porous crystalline networks. The crystal structure of Zr terephthalate MOF UiO-66 was reported in 2008<sup>5</sup> and revised in 2011,<sup>6</sup> solved from powder X-ray diffraction (PXRD), extended X-ray absorption fine structure (EXAFS), and periodic density functional theory (DFT) calculations. This approach was repeated in 2012 for UiO-67.<sup>7</sup>

From thermogravimetric analysis (TGA) and adsorption measurements, it is known that Zr-MOFs are often imperfect in the sense that they have missing linkers, and this is related to stability and other properties.<sup>8–10</sup> The structural models presented so far for these materials, though broadly accurate, do not fully explain some of the properties of the two MOF materials, e.g., unexpected decomposition at low temperatures or in the presence of water. Here we present a model based on single-crystal synchrotron XRD data of exceptionally high quality, showing clear evidence of structural defects caused by missing linkers.

Single crystal X-ray diffraction is able to provide a very accurate picture of electron density, and thus atomic structure, in three dimensions (Figure 1). Although there are a few reported structures for Zr-MOFs,<sup>11–13</sup> these are not of sufficient quality to determine detailed structural features.

Single crystals of UiO-66 and UiO-67 were synthesized by a modification of a previously reported method, using benzoic acid as a monodentate ligand to inhibit crystal seeding.<sup>14</sup> The Erlenmeyer flasks used in the syntheses were submerged in 2.0 M  $\text{KOH}_{(\text{aq})}$  overnight prior to use in the reaction, to further

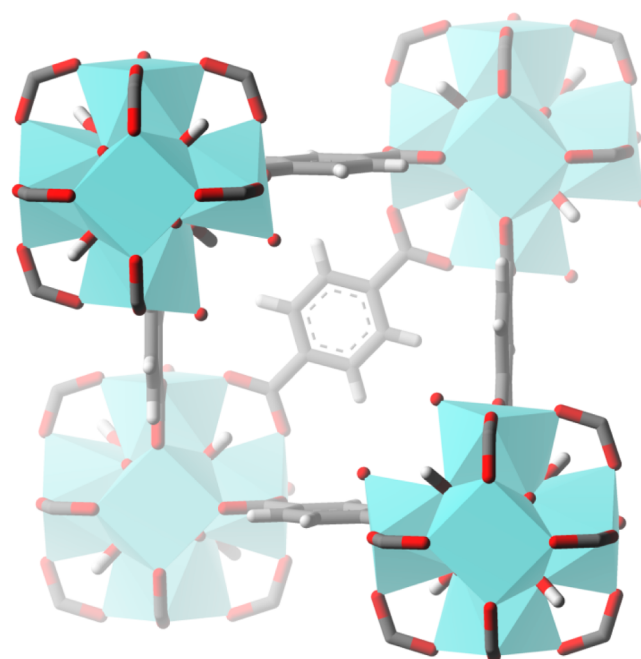


**Figure 1.** Partial unit cell of UiO-66 showing a missing linker defect and different positions of  $\mu^3\text{-O}$  and  $\mu^3\text{-OH}$ .

inhibit seeding on the glass surface. This resulted in well separated single crystals attached to the inclining surfaces of the synthesis flasks, while the majority of the product formed a

**Received:** September 16, 2014

**Published:** October 1, 2014

membrane of intergrown crystals on the flask bottom (Figure 2). A complete description can be found in the Supporting Information.

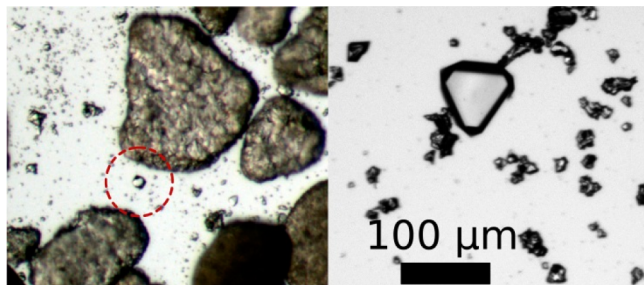


**Figure 2.** Optical micrographs with the same degree of magnification of single crystals of UiO-66 (left) and UiO-67 (right).

Single crystal X-ray diffraction experiments were carried out at beamline I911-3 at the MAX2 synchrotron at MaxLab, Lund,<sup>15</sup> working with  $\lambda = 0.760$  Å.

The single crystals of UiO-67 were heated to 150 °C for 1 h before measurement to remove excess solvent from the pores. The measurements were carried out at 100 K, on two separate crystals of UiO-66 and two separate crystals from two separate syntheses of UiO-67. The largest UiO-66 single crystals were in the range of 5–10  $\mu\text{m}$ , while crystals of UiO-67 up to 75  $\mu\text{m}$  could be found (Figure 2).

The crystal structures were refined without imposing restraints. We allowed oxygen atoms with freely refining occupancy factor to occupy the pores, to model disordered electron density, thus avoiding the use of algorithms such as SQUEEZE<sup>16</sup> in the main refinements. The results are summarized in Table 1.

**Table 1. Structure Refinement Summary of UiO-66 and UiO-67, Both Data Sets Complete to 0.71 Å Resolution, and Space Group  $Fm\bar{3}m$**

compd	UiO-66	UiO-67
<i>a</i>	20.7465(2) Å	26.8809(3) Å
data/parameters/restraints	739/53/0	1514/55/0 Å
Zr- $\mu^3$ -O	2.064(3) Å	2.059(2) Å
Zr- $\mu^3$ -OH	2.254(5) Å	2.256(8) Å
<i>R</i> <sub>i</sub> (all data)	2.44%	2.32%

The refinements show that the samples have hydroxylated clusters, with 0.5 occupancy of both  $\mu^3$ -O and  $\mu^3$ -OH in all measurements, the positions of which agree with previously reported calculations.<sup>17</sup> The four protons are also required for the charge balance of the cluster. This result is expected since the dehydration of the cluster occurs at 220 °C. The  $\mu^3$ -O site is closer to the centroid of the  $\text{Zr}_6$  octahedron by  $\sim 0.62$  Å (Figure 3). This is consistent with previous EXAFS data and periodic DFT studies.

The linker occupancy of each structure was allowed to refine freely. In UiO-66, it converged to 73% in both independent refinements and in UiO-67 to close to 100%.

Large irregularities in the electron density were observed around the carboxylate oxygen of UiO-66. The model was made with two separate oxygen atoms to fit this; one with the same occupancy as the linker (called  $\text{O}_{\text{carboxylate}}$ ) and one with inverse occupancy (called  $\text{O}_{\text{defect}}$ ) (Figure 4). It was not

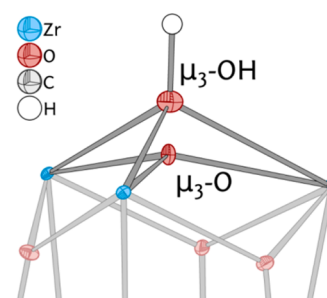


**Figure 3.** Positions of  $\mu^3$ -O and  $\mu^3$ -OH in the  $\text{Zr}_6\text{O}_4(\text{OH})_4$  cluster.

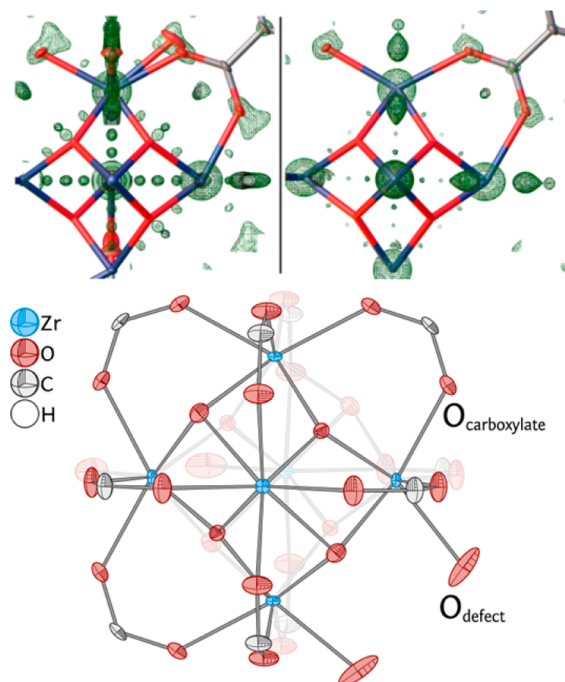


**Figure 4.**  $F_{\text{obs}}$  electron density map drawn around a stick model of UiO-66 (top left) and UiO-67 (top right), and a cluster containing both configurations of carboxylate oxygen (bottom).

possible to further model the chemical structure of the range of molecules, which may occupy the  $\text{O}_{\text{defect}}$  position, and they are assumed to be a mixture of hydroxide, water, and DMF or other coordinating solvents. This finding explains the difference in the intensity of the second shell Zr–Zr peak in the EXAFS data collected on UiO-66 and UiO-67, in terms of the structural disorder of the  $\text{Zr}_6\text{O}_4(\text{OH})_4$  octahedron induced by missing ligands.<sup>18</sup>

Although the linker occupancy in UiO-66 is found to be about 73%, this figure may be inaccurate due to correlation between occupancy and three thermal factors, and the partial overlap between the defect and carboxylate position.

Although benzoic acid was used in large amounts in the synthesis of both materials, it is not incorporated into the structure. This would have caused large thermal vibrations of the carbons para to the carboxylic acid group, but no such features are observed in the crystal structures. The relatively large thermal displacement parameters of  $\text{O}_{\text{defect}}$  can be attributed to the defects being multiple species and the proximity to  $\text{O}_{\text{carboxylate}}$ .

TGA and PXRD results show slight deviations in linker occupancy from the SC-XRD structures, which indicate minor

differences between the single crystals and the bulk sample. The intergrown membrane of crystals in the bulk sample had different growth conditions from those of the single crystals on the flask wall, and there may be other solids present in the sample, such as amorphous Zr terephthalates, oxides, and hydroxides, which cannot easily be separated from the MOF. These results are described in detail in the Supporting Information.

Diffuse scattering was observed on the expected positions of the symmetry-forbidden diffraction peaks (1 0 0), (1 1 0), and (5 0 0), suggesting that there is some long-range order of the defects and/or missing clusters. This has recently been discussed in detail by Cliffe et al.<sup>19</sup>

In conclusion, we have determined the structure of Zr-MOFs UiO-66 and UiO-67 to an unprecedented degree of accuracy, disentangling the  $\mu_3$ -O position of the prismatic faces of the Zr<sub>6</sub> octahedron into two distinct  $\mu_3$ -O and  $\mu_3$ -OH, with occupancy of 0.5 each, and having Zr–O and Zr–OH distances in agreement with those obtained from EXAFS data and periodic DFT studies. The use of benzoic acid in the synthesis prevents the formation of chloride-terminated cluster defects previously observed but does not affect the amount of missing linkers in UiO-66. The missing linkers, along with key differences in the location and thermal motion of the defect oxygen atoms compared to those from linker molecules, explain, on a structural ground, the origin of the different thermal stability of UiO-66 samples prepared with different synthesis methods.<sup>6,10</sup> This point is of fundamental importance for several possible applications of this class of materials, including their functionalized forms. The results are a significant step toward understanding the stability and behavior of these exciting but complex materials.

## ■ ASSOCIATED CONTENT

### Supporting Information

Further details of synthesis, experimental methods, and crystal structure files. This material is available free of charge via the Internet at <http://pubs.acs.org>.

### Accession Codes

The crystal structures are submitted to The Cambridge Crystallographic Data Centre with identifiers CCDC 1018045 and 1018032 and can be obtained free of charge from <http://www.ccdc.cam.ac.uk/cgi-bin/catreq.cgi>.

## ■ AUTHOR INFORMATION

### Corresponding Author

\*E-mail: [k.p.lillerud@kjemi.uio.no](mailto:k.p.lillerud@kjemi.uio.no).

### Notes

The authors declare no competing financial interest.

## ■ ACKNOWLEDGMENTS

This work is part of inGAP and CLIMIT, which receive financial support from the Norwegian Research Council under contract Nos. 174893 and 215735, respectively. The authors would like to thank Folmer Fredslund at MaxLAB for his support at the beamline.

## ■ REFERENCES

- (1) Fei, H.; Shin, J.; Meng, Y. S.; Adelhardt, M.; Sutter, J.; Meyer, K.; Cohen, S. M. *J. Am. Chem. Soc.* **2014**, *136*, 4965–4973.
- (2) Manna, K.; Zhang, T.; Lin, W. *J. Am. Chem. Soc.* **2014**, *136*, 6566–6569.
- (3) Wang, C.; Volotskova, O.; Lu, K.; Ahmad, M.; Sun, C.; Xing, L.; Lin, W. *J. Am. Chem. Soc.* **2014**, *136*, 6171–6174.
- (4) Furukawa, H.; Gandara, F.; Zhang, Y.-B.; Jiang, J.; Queen, W. L.; Hudson, M. R.; Yaghi, O. M. *J. Am. Chem. Soc.* **2014**, *136*, 4369–4381.
- (5) Hafizovic, J. C.; Jakobsen, S.; Olsbye, U.; Guillou, N.; Lamberti, C.; Bordiga, S.; Lillerud, K. P. *J. Am. Chem. Soc.* **2008**, *130*, 13850–13851.
- (6) Valenzano, L.; Civalieri, B.; Chavan, S.; Bordiga, S.; Nilsen, M. H.; Jakobsen, S.; Lillerud, K. P.; Lamberti, C. *Chem. Mater.* **2011**, *23*, 1700–1718.
- (7) Chavan, S.; Vitillo, J. G.; Gianolio, D.; Zavorotynska, O.; Civalieri, B.; Jakobsen, S.; Nilsen, M. H.; Valenzano, L.; Lamberti, C.; Lillerud, K. P.; Bordiga, S. *Phys. Chem. Chem. Phys.* **2012**, *14*, 1614–1626.
- (8) Vermoortele, F.; Bueken, B.; Le Bars, G.; Van de Voorde, B.; Vandichel, M.; Houthoofd, K.; Vimont, A.; Daturi, M.; Waroquier, M.; Van Speybroeck, V.; Kirschhock, C.; De Vos, D. E. *J. Am. Chem. Soc.* **2013**, *135*, 11465–11468.
- (9) Wu, H.; Chua, Y. S.; Krungleviciute, V.; Tyagi, M.; Chen, P.; Yildirim, T.; Zhou, W. *J. Am. Chem. Soc.* **2013**, *135*, 10525–10532.
- (10) Shearer, G. C.; Chavan, S. M.; Ethiraj, J.; Vitillo, J. G.; Svelle, S.; Olsbye, U.; Lamberti, C.; Bordiga, S.; Lillerud, K. P. *Chem. Mater.* **2014**, *26*, 4068–4071.
- (11) Bon, V.; Senkovskyy, V.; Senkovska, I.; Kaskel, S. *Chem. Commun.* **2012**, *48*, 8407–8409.
- (12) Zhang, M.; Chen, Y.-P.; Bosch, M.; Gentle, T.; Wang, K.; Feng, D.; Wang, Z. U.; Zhou, H.-C. *Angew. Chem., Int. Ed.* **2014**, *53*, 815–818.
- (13) Morris, W.; Voloskiy, B.; Demir, S.; Gandara, F.; McGrier, P. L.; Furukawa, H.; Cascio, D.; Stoddart, J. F.; Yaghi, O. M. *Inorg. Chem.* **2012**, *51*, 6443–6445.
- (14) Schaate, A.; Roy, P.; Godt, A.; Lippke, J.; Waltz, F.; Wiebcke, M.; Behrens, P. *Chem.—Eur. J.* **2011**, *17*, 6643–6651.
- (15) Ursby, T.; Unge, J.; Appio, R.; Logan, D. T.; Fredslund, F.; Svensson, C.; Larsson, K.; Labrador, A.; Thunnissen, M. M. G. M. *J. Synchrotron Radiat.* **2013**, *20*, 648–653.
- (16) Spek, A. L. *J. Appl. Crystallogr.* **2003**, *36*, 7–13.
- (17) Shearer, G. C.; Forselv, S.; Chavan, S.; Bordiga, S.; Mathisen, K.; Bjorgen, M.; Svelle, S.; Lillerud, K. P. *Top. Catal.* **2013**, *56*, 770–782.
- (18) Gianolio, D.; Vitillo, J. G.; Civalieri, B.; Bordiga, S.; Olsbye, U.; Lillerud, K. P.; Valenzano, L.; Lamberti, C. *J. Phys.: Conf. Ser.* **2013**, *430*, 012134.
- (19) Cliffe, M. J.; Funnell, N. P.; Goodwin, A. L.; Wan, W.; Zou, X.; Chater, P. A.; Kleppe, A. K.; Wilhelm, H.; Tucker, M. G.; Coudert, F.-X. *Nat. Commun.* **2014**, *5*, 4176.